Back Electron Transfer at TiO$_2$ Nanotube Photoanodes in the Presence of a H$_2$O$_2$ Hole Scavenger

Heng Zhu,[†] Shicheng Yan,[†] Zhaosheng Li,[†] Zhigang Zou[†,‡]*

[†] Eco-Materials and Renewable Energy Research Center (ERERC), Collaborative Innovation Center of Advanced Microstructures, College of Engineering and Applied Sciences, Nanjing University, No. 22, Hankou Road, Nanjing, Jiangsu 210093, P. R. China

[‡] Jiangsu Key Laboratory for Nano Technology, National Laboratory of Solid State Microstructures, Department of Physics, Nanjing University, No. 22, Hankou Road, Nanjing, Jiangsu 210093, P. R. China

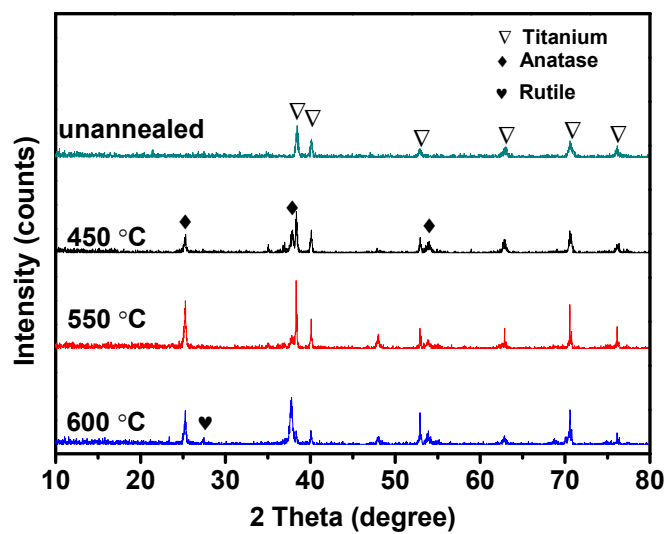Corresponding authors: E-mail: yscfei@nju.edu.cn

Figure S1. XRD patterns of the as-grown TiO$_2$ nanotube arrays before and after annealing in air at 450，550 and 600 ^{o}C for 2 h. The samples obtained by anodic oxidation were amorphous without annealing in air. If the samples annealed in air at 600 ^{o}C, the rutile phase appears. In this study, the annealed temperature was 450 ^{o}C for obtaining a single-phase anatase TiO$_2$.
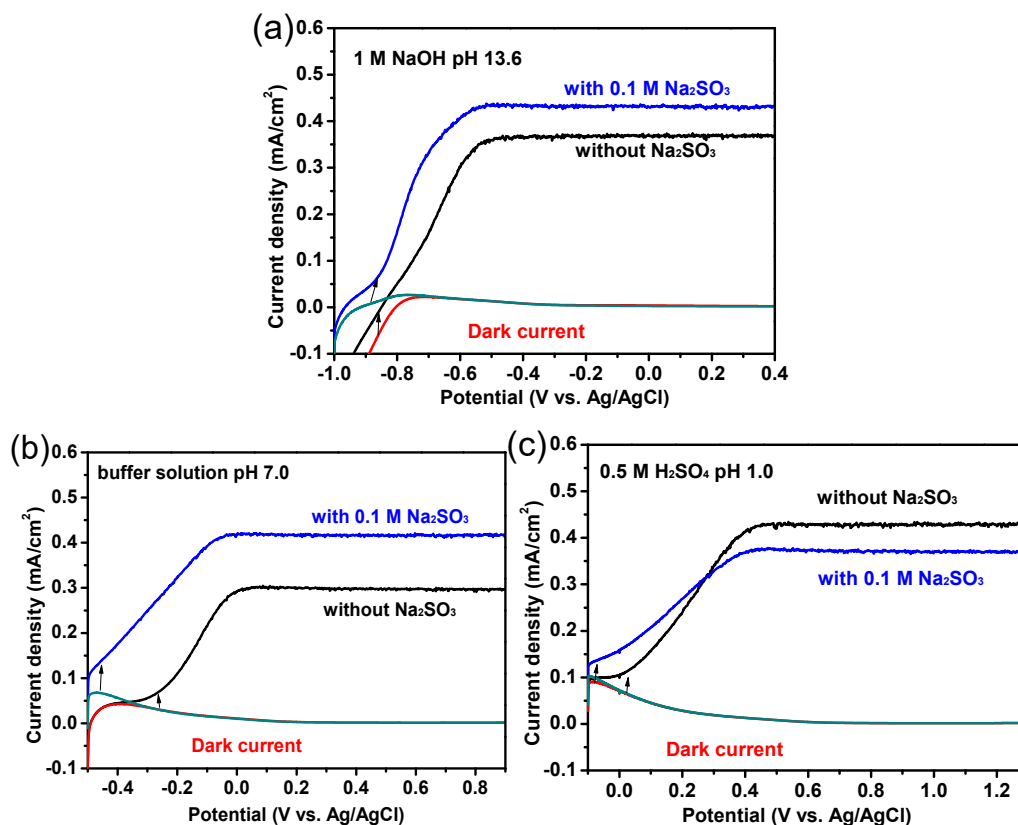
Figure S2. Effect of sulfite ions on photocurrent density versus potential curves for TiO_2 nanotube electrodes. Electrolyte: (a) 1 M NaOH solution, pH 13.6, (b) phosphate buffer solution, pH 7.0, (c) 0.5 M H_2SO_4 solution, pH 1.0. Scan rate 20 mV s^{-1}. The hole scavenger SO_3^{2-} was oxidized more easily than water. In the alkaline and neutral electrolytes, in presence of the SO_3^{2-}, the photocurrent increased, indicating that the SO_3^{2-} is the effective hole scavenger. However, in acidic solution, after adding of SO_3^{2-}, the photocurrent decreased slightly due to that the SO_3^{2-} decomposition in strong acid into SO_2, probably affecting the adsorption of H_2O on TiO_2.
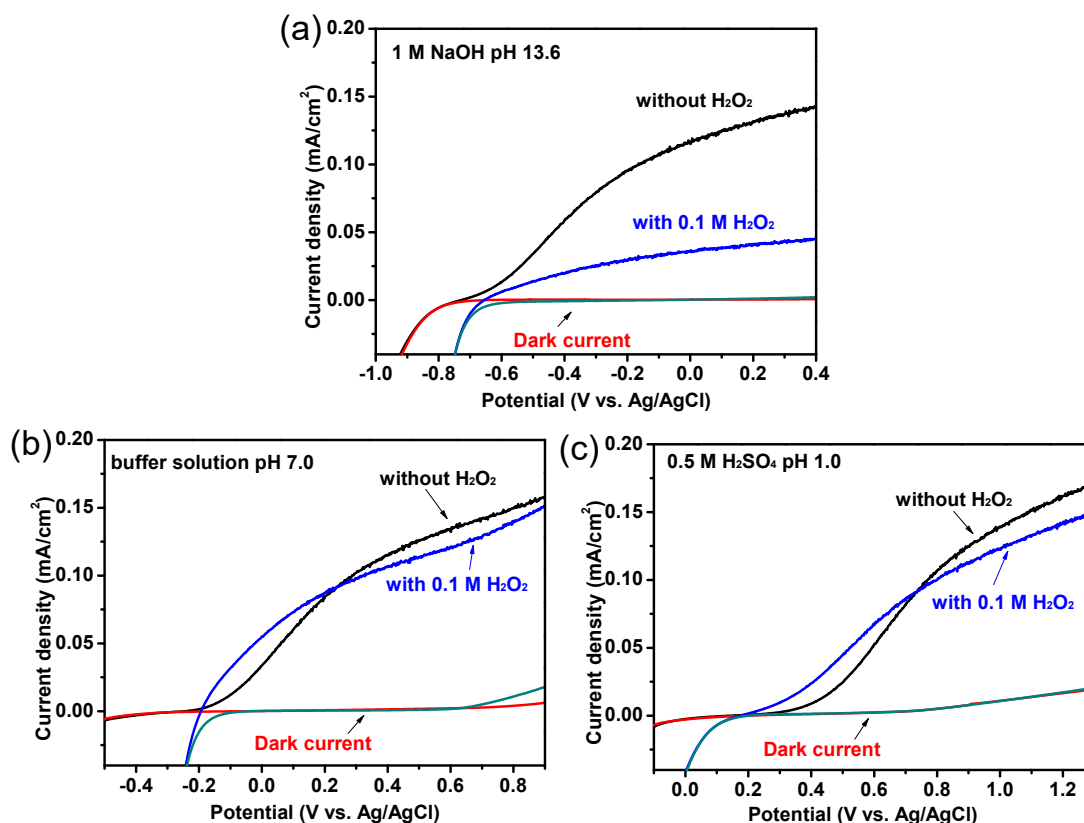
Figure S3. Effect of hydrogen peroxide on photocurrent density versus potential curves for compact TiO_2 plate electrodes. Electrolyte: (a) 1 M NaOH solution, pH 13.6, (b) phosphate buffer solution, pH 7.0, (c) 0.5 M H_2SO_4 solution, pH 1.0. Scan rate 20 mV s^{-1}. The compact TiO_2 film was obtained by oxidizing the chemically polished Ti sheets in air at 450 °C for 2 h. In alkaline solution the hydrogen peroxide makes the saturated photocurrent of the compact TiO_2 plate electrodes decrease dramatically. It indicates that the surface states also exist on the compact TiO_2 plate electrode. An obvious difference is that the saturated photocurrent on compact TiO_2 plate electrodes is lower than that on TiO_2 nanotube electrodes, due to the significant difference in their semiconductor-electrolyte contact area. Therefore, we can believe that the H_2O_2-related saturated photocurrent decrease is dependent on the surface states of electrodes, independent on the microstructure of electrodes.
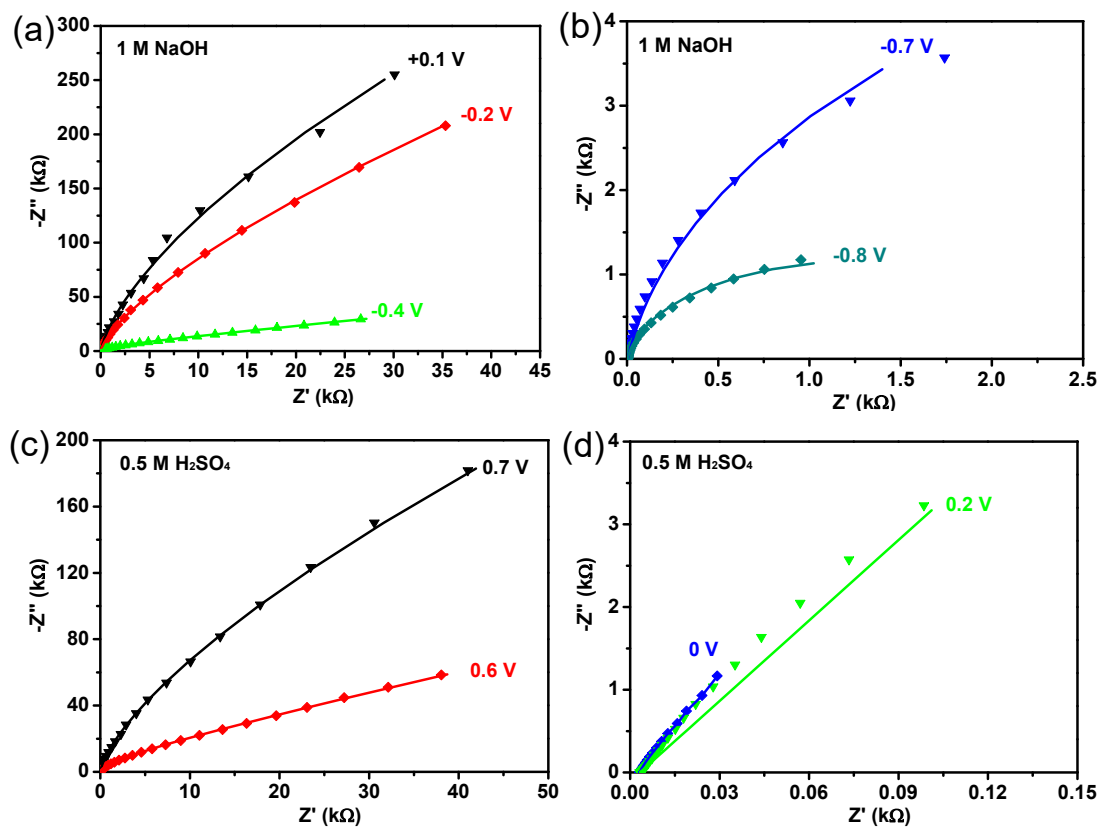
Figure S4. Impedance diagrams (Nyquist representation) of the TiO$_2$ nanotube electrodes in the dark (a,b) in 1 M NaOH and (c,d) 0.5 M H$_2$SO$_4$ electrolytes. The solid lines were the fitting curves according to the equivalent circuit. Performing in potentiostatic conditions, frequencies ranging from 0.1 Hz to 100 KHz, using a 10 mV sinusoidal potential modulation.
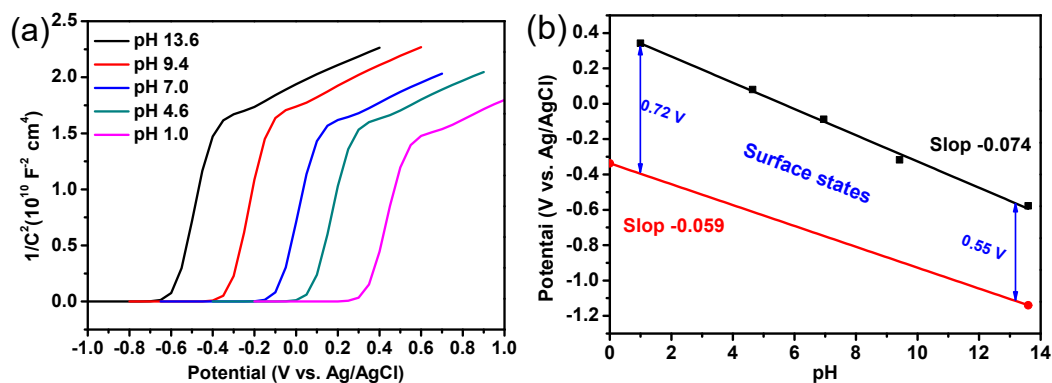
Figure S5. (a) Mott-Schottky plots collected at frequency of 1 kHz for the TiO$_2$ electrode in the dark in different pH electrolytes. (b) Dependence of initial potential for occurrence of surface states for TiO$_2$ nanotube electrodes on pH of electrolytes (black line). The dependence of theoretical flat band potential on pH for TiO$_2$ electrode was also shown for comparison (red line). The theoretical flat band potential should increase by ~59 mV per pH in accord with the Nernst equation. However, the increase step of initial potential for occurrence of surface states is about 74 mV per pH, probably resulting from the effect of surface states on the potential-determining ions.
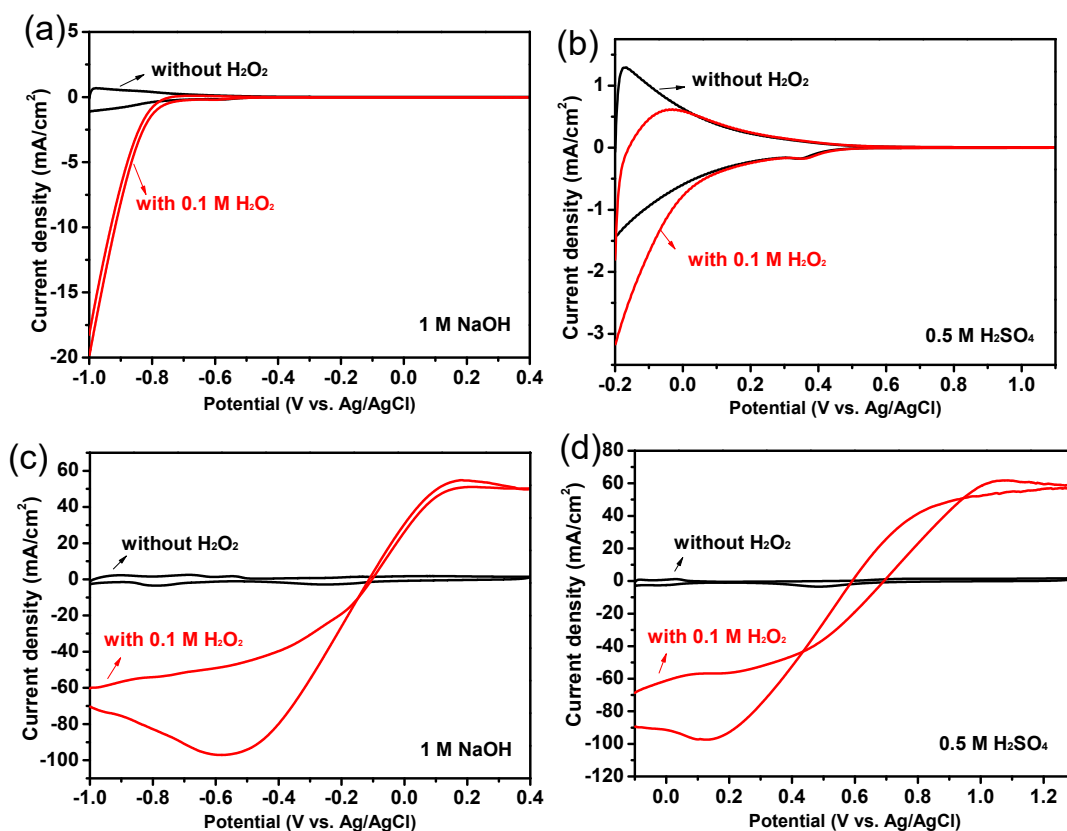
Figure S6. Cyclic voltammogram of TiO_2 nanotube electrodes in (a) 1 M NaOH solution (pH 13.6) with and without H_2O_2, (b) 0.5 M H_2SO_4 solution (pH 1.0) with and without H_2O_2. Cyclic voltammogram of Pt electrode in (c) 1 M NaOH solution (pH 13.6) with and without H_2O_2, (d) 0.5 M H_2SO_4 solution (pH 1.0) with and without H_2O_2. Scan rate 500 mV s^{-1}. The cathodic current increased dramatically, when adding hydrogen peroxide into 1 M NaOH solution. From Figurea and b, we can know that the hydrogen peroxide was reduced more easily in alkaline solution than in acidic solution at TiO_2 nanotube electrodes. We also do the experiments at Pt electrode. However the phenomenon at Pt electrode is different with that at TiO_2 nanotube electrodes. From Figure c and d, it seems that hydrogen peroxide shows almost the same reduction property both in alkaline and acidic solution, indicating that the mechanism of the reduction of H_2O_2 at Pt and TiO_2 nanotube electrodes are very different.

Table S1. The values of standard electrode potentials are given below in volts relative to the standard hydrogen electrode

Oxidant	$\rightleftharpoons$	Reductant	E^o (V)
$2H^+ + 2e^-$	$\rightleftharpoons$	$H_2(g)$	0.0000
$SO_4^{2-} + 2H^+ + 2e^-$	$\rightleftharpoons$	$SO_3^{2-}(aq) + H_2O$	+0.17
$O_2(g) + 2H^+ + 2e^-$	$\rightleftharpoons$	$H_2O_2(aq)$	+0.68
$O_2(g) + 4H^+ + 4e^-$	$\rightleftharpoons$	$2H_2O$	+1.229
$H_2O_2(aq) + 2H^+ + 2e^-$	$\rightleftharpoons$	$2H_2O$	+1.78

Legend: (aq) – aqueous; (s) – solid

Table S2. Fitting parameters obtained by using the equivalent circuit proposed in Figure 4c and d.

Electrolytes	Potential (V vs .Ag/AgCl)	CPE Q ($\mu\Omega^{-1}\,s^n$)	CPE n	R_s (Ω)	$R_s + R_{trap}$ (Ω)	$R_{ct,bulk}$ (KΩ)	$R_{ct,trap}$ (KΩ)
	-0.9	1400	0.94		3.02		10.6
	-0.7	388	0.93		4.00		13.3
1 M NaOH	-0.3	7.87	0.96	3.00		367.5	
	-0.1	6.44	0.98	3.06		2002.3	
	0	6.21	0.98	3.07		2481.1	
	-0.2	3330	0.98		3.08		20.4
	0	1320	0.98		3.11		31.5
0.5 M H$_2$SO$_4$	0.2	469	0.98		3.40		69.7
	0.6	11.1	0.93	2.96		98.7	
	0.8	6.69	0.98	3.15		1839.2	